

**AUTHORS:**

Alison F. Ridel<sup>1</sup>   
 Fabrice Demeter<sup>2,3</sup>   
 Ericka N. L'Abbé<sup>1</sup>   
 Dirk Vandermeulen<sup>1,4</sup>   
 Anna C. Oettlé<sup>1,5</sup> 

**AFFILIATIONS:**

<sup>1</sup>Department of Anatomy, Faculty of Health Sciences, University of Pretoria, Pretoria, South Africa  
<sup>2</sup>Lundbeck Foundation GeoGenetics Centre, Globe Institute, University of Copenhagen, Copenhagen, Denmark  
<sup>3</sup>Department of Man and the Environment, Museum of Man, Paris, France  
<sup>4</sup>Center for Processing Speech and Images (PSI), Department of Electrical Engineering (ESAT), KU Leuven, Leuven, Belgium  
<sup>5</sup>Department of Anatomy, School of Medicine, Sefako Makgatho Health Sciences University, Pretoria, South Africa

**CORRESPONDENCE TO:**

Alison Ridel

**EMAIL:**

alison.ridel@up.ac.za

**DATES:**

**Received:** 15 Dec. 2021  
**Revised:** 23 Aug. 2023  
**Accepted:** 27 Feb. 2024  
**Published:** 28 May 2024

**HOW TO CITE:**

Ridel AF, Demeter F, L'Abbé EN, Vandermeulen D, Oettlé AC. Shape analysis of the nasal complex among South African groups from CBCT scans. *S Afr J Sci.* 2024;120(5/6), Art. #12972. <https://doi.org/10.17159/sajs.2024/12972>



**ARTICLE INCLUDES:**

- Peer review
- Supplementary material

**DATA AVAILABILITY:**

- Open data set
- All data included
- On request from author(s)
- Not available
- Not applicable

**EDITORS:**

Pascal Bessong   
 Shane Redelinghuys 

**KEYWORDS:**

human variation of South African groups, cone-beam computer tomography scans, geometric morphometric methods, South African standard facial reconstruction methods

**FUNDING:**

None

© 2024. The Author(s). Published under a Creative Commons Attribution Licence.

# Shape analysis of the nasal complex among South African groups from CBCT scans

Three-dimensional (3D) anatomical extraction techniques could help the forensic anthropologist in a precise and inclusive assessment of biological phenotypes for the development of facial reconstruction methods. In this research, the nose morphology and the underlying hard tissue of two South African populations were studied. To this end, a 3D computer-assisted approach based on an automated landmarking workflow was used to generate relevant 3D anatomical components, and shape discrepancies were investigated using a data set of 200 cone-beam computer tomography (CBCT) scans. The anatomical landmarks were placed on the external nose and the mid-facial skeleton (the nasal bones, the anterior nasal aperture, the zygoma, and the maxilla). Shape differences related to population affinity, sex, age, and size were statistically evaluated and visualised using geometric morphometric methods. Population affinity, sexual dimorphism, age, and size affect the nasal complex morphology. Shape variation in the mid-facial region was significantly influenced by population affinity, emphasising that shape variability was specific to the two population groups, along with the expression of sexual dimorphism and the effect of ageing. In addition, nasal complex shape and correlations vary greatly between white and black South Africans, highlighting a need for reliable population-specific 3D statistical nose prediction algorithms.

**Significance:**

- 3D anatomical structures were acquired and extracted from 200 CBCT scans of modern South Africans.
- Geometric morphometric methods were applied.
- Soft- and hard-tissue nasal complex morphology vary across South African groups.

## Introduction

The human phenotype is a suite of apparent morphological characteristics of a person, which are dependent on the expression of genes (genotype) and the environment. Today, with the development of new technologies, biological anthropologists are able to extensively and intensively collect these quantitative phenotypic data for evaluating variation within and between populations. These population-specific data are often applied in the forensic sciences (e.g. biological profile and facial reconstruction), medicine (e.g. orthopaedics, prosthetics, and plastic surgery), and education.<sup>1</sup> Today, modern 3D digital imaging methods provide researchers with extensive in vivo and non-invasive databases of 3D representations of the face (soft and hard tissues).

Ultrasound<sup>2</sup>, magnetic resonance imaging<sup>3</sup>, computer tomography (CT), and cone-beam computed tomography (CBCT)<sup>4,5</sup> scans are examples of digital imaging modalities that provide an optimal means for capturing information on facial appearance within a population.

However, standard approaches for working with big data, as represented in readily available 3D images from public and private hospitals, have not grown as fast as the research ideas for applying variation found among phenotypic features within a population to real-world outcomes. With knowledge of both soft tissue and hard tissue, we can now use this understanding of variation in forensic anthropology, such as quantifiable biological variation among population groups, which helps provide an accurate biological profile.<sup>6</sup> Precise quantification of anatomical shape from digital images is essential for evaluating phenotypic variation and applying this knowledge to evolutionary processes, medicine, and the forensic sciences. Nevertheless, standard guidelines for how to collect data from 3D images need to be considered. Traditionally, in biological anthropology, this has been accomplished by collecting: (1) linear distances; (2) measurements between manually set landmarks; or (3) shape data by assessing the entire array of landmarks using geometric morphometric models (GMM). However, the manual placement of anatomical landmarks is time-consuming, prone to significant intra- and inter-observer error, and remains challenging to standardise in practice.<sup>1,5,7</sup> To avoid the problems of manually placing landmarks by multiple operators, the utilisation of automatic anatomical extraction techniques, such as automatic landmarking, is more suitable for analysing large data sets.<sup>5,8</sup> Today, the utilisation of GMM instead of linear distances is fostered for phenotypic variation analysis because it allows the extraction of size-free shape variables to elucidate the patterns of shape variation more satisfactorily. Using a dense configuration of landmarks will also give a more comprehensive evaluation of the morphology and is preferable for applications that need extensive knowledge of the biological phenotypic changes, such as estimating a biological profile in forensic anthropology.

There are discrete patterns of biological variation among humans, such as clinal phenotypic variability, which is often driven by social and cultural aptitudes and noticed at geographical distances.<sup>9,9</sup> Numerous bioanthropological investigations on population affinity related shape changes have proven the effect of environmental influences on nose shape<sup>10</sup>, emphasising the fundamental premise that the external nose shape and anterior nasal aperture are pivotal in climate adaptation.<sup>10</sup> From the scientific literature, discrete morphological differences have already been noticed between all South African groups.<sup>11-13</sup> Numerous osteometric investigations have indicated that some



mid-face features, such as alveolar prognathism and nasal breadth, are population affinity related morphological variations.<sup>11-13</sup>

Identification of a person from their skeletal remains is problematic in many developing-world countries, including South Africa.<sup>14</sup> Due to social and political situations, standard identification procedures such as fingerprinting and DNA comparisons are not always applicable. Furthermore, many South African people do not have identification documents. Further compounding these circumstances is that many migrants are coming into the country from all over Africa. Consequently, this context necessitates using creative and cost-effective technologies such as facial reconstruction techniques to assist in creating visual representations for the prospective identification of deceased family members.

Craniofacial reconstruction (CFR) is defined as the presumed morphological correlation between soft tissue and underlying hard tissue. Three categories of facial reconstruction techniques exist: 2D, 3D manual facial reconstruction, and 3D computer-based facial reconstruction. The scientific community acknowledges that manual CFR techniques necessitate a high level of sculptural and anatomical proficiency and remain subjective in practice.<sup>15,16</sup> Today, researchers in the field of CFR utilise technological advances such as computer science and medical imaging to develop alternative computer-based CFR methods to improve the objectivity of facial reconstructions during criminal investigations.<sup>4,5,17</sup> Computers are more impartial and consistent than forensic artists.<sup>17</sup> The computer incorporates all modelling assumptions and provides identical output data repeatedly.<sup>17</sup> Furthermore, some techniques may be automated, such as developing several reconstructions from the same target skull based on various modelling assumptions (e.g. biological variation).<sup>17</sup> The history and evolution of craniofacial reconstruction methods and their applications have shown the extent of human diversity within and across communities, laying the foundations for the current development of accurate population-specific standards.

The presumptive identification of an unknown person is predicated on the existence of quantifiable phenotypic variations and the relationship of these variations to the individual's socio-cultural identity.<sup>18</sup> Socio-cultural identity in South Africa is based on the cohesive social classifications imposed on people during the apartheid period, notably 'White', 'Black', 'Coloured', and 'Indian'. People in these groups hail from vastly distinct

geographical environments and have already exhibited various cultural and biological characteristics. For instance, 'white' people mainly descend from European immigrants, including Dutch, German, British, and French.<sup>11</sup> In comparison, the modern 'black' population groups are the descendants of Sotho, Venda, Nguni, and Shangaan-Tsonga migrants who came to southern Africa due to Bantu language tribes migrating from central and western Africa.<sup>18,19</sup>

In addition, assortative mating among the **modern** South African **population** enhanced the already **substantial** biological variability between groups. Consequently, it fostered the persistence of skeletal variation to the extent that forensic anthropologists may categorise an unknown person into four major socially identifiable categories: black, coloured, Indian or white South Africans.<sup>20</sup>

In this study, we aimed to establish standardised and comprehensive morphological representations of the nasal complex (mid-facial skeleton and external nose) within two South African population groups from an extensive CBCT database that can be used to examine phenotypic diversity. In this research, we propose a reliable assessment of morphological variations attributable to variables (population affinity, age, sex, and allometry) by applying an automated landmarking workflow<sup>5,8</sup> and GMM.

## Materials and methods

A retrospective and anonymised database of CBCT scans was collected from two South African institutions: the Life Groenkloof Hospital and the Oral and Dental Hospital, Pretoria, South Africa. All CBCT scans were acquired using a CBCT scanning modality with the following specifications: 90 kV, 11.2 mA, 0.4 mm voxel size, and 230 × 260 mm field of view. Subjects were excluded if they presented with any condition that could affect the morphology of the face (e.g. orthodontic treatment, pathological conditions, facial asymmetry, or any facial interventional reconstructive surgery), resulting in 200 usable scans. Therefore 200 adult South Africans with an average age of 40.51 years (SD: 16.17), of whom 100 were black South Africans (33 women, 67 men) and 100 were white South Africans (65 women, 35 men), were selected from the available database for this study. Ethical approval (No: 301/2016) to conduct this research was obtained from the Main Research Ethics Committee of the Faculty of Health Sciences at the University of Pretoria in South Africa.

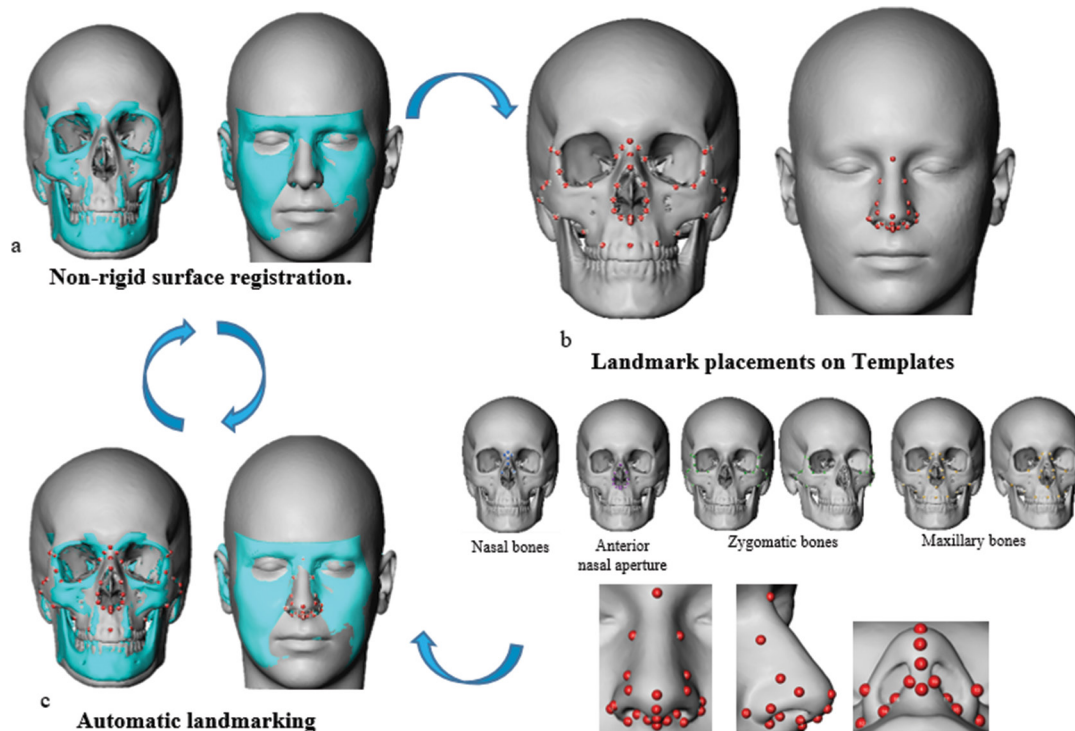


**Figure 1:** Automatic landmarking workflow from Ridet et al. used in this study: (a) non-rigid surface registration process; (b) templates generation and landmarks positioning; and (c) automatic landmarking.<sup>5,8</sup>

We used the MeVisLab v. 2.7.1 software to create the triangular surface mesh and carry out anatomical extraction. Relevant anatomical structures in 3D were obtained and retrieved using an already tested and published automatic dense landmarking workflow.<sup>5,8</sup> The automated landmarking workflow used is depicted in Figure 1.

Biological landmarks were respectively placed on the external nose (soft tissue) and the facial skeleton (hard tissue) following the definition in facial approximation literature<sup>4,21</sup> (Figure 1b). A total of 21 capulometric landmarks were placed to capture the external nose morphology. Five craniometric landmarks were recorded on the nasal bones and eight craniometric landmarks on the anterior nasal aperture. On the zygomatic bone, nine craniometric landmarks were placed, whereas, on the maxillary bone, ten craniometric landmarks (two median and eight bilateral pairs) were positioned. A total of 41 craniometric and 21 capulometric

landmarks were recorded for 3D manual facial reconstruction and 3D computer-based facial reconstruction, respectively. Table 1 shows the definition and reproducibility of craniometric landmarks placed automatically and used in this study.

In this research, all statistical analyses were carried out using R studio for Windows<sup>22</sup> version 1.0.44-@2009-2016. The complete sample (400 3D reconstructions) was subjected to a test of the repeatability of the digitisation in terms of inter- and intra-observer errors using the dispersion<sup>5</sup> for each landmark and specimen. The dispersion was used to assess the reproducibility of digitisation across and between observers (inter- and intra-observer) for the complete sample (400 3D reconstructions) based on the utilisation of automatic landmarking. The mean Euclidean distance between the landmark and the mean of the (x,y,z)-landmark coordinates across all observations for each specimen is used to measure dispersion.

**Table 1:** Definition and reproducibility of craniometric landmarks placed automatically and used in this study<sup>4,21</sup>

	Landmarks	Abbreviation	Nature	Definition
<b>Craniometric</b>				
1	Nasion	n	M	Intersection of the nasofrontal sutures in the median plane.
2	Mid-nasal	mn	M	Midline point on the internasal suture midway between the nasion and rhinion.
3	Rhinion	rhi	M	Most rostral (end) point on the internasal suture. Cannot be determined accurately if nasal bones are broken distally.
4	Nasospinale	ns	M	The point where a line drawn between the inferior most points of the nasal aperture crosses the median plane. Note that this point is not necessarily at the tip of the nasal spine.
5	Subspinale b	ss	M	The deepest point seen in the profile view below the anterior nasal spine (orthodontic point A).
6	Akanthion	ak	M	Most anterior midline point of the nasal spine.
7	Prosthion	pr	M	Median point between the central incisors on the anterior most margin of the maxillary alveolar rim.
8/9	Zygotemporale superior	zts	B	Most superior point of the zygomatico-temporal suture.
10/11	Zygotemporale inferior	zti	B	Most inferior point of the zygomatico-temporal suture.
12/13	Jugale	ju	B	Vertex of the posterior zygomatic angle, between the vertical edge and horizontal part of the zygomatic arch.
14/15	Frontomalare temporale	fmt	B	Most lateral part of the zygomaticofrontal suture.
16/17	Frontomalare orbitale	fmo	B	Point on the orbital rim marked by the zygomaticofrontal suture.
18/19	Nasomaxillofrontale	nmf	B	Point at the intersection of the frontal, maxillary, and nasal bones.
20/21	Ectoconchion	ec	B	Lateral point on the orbit at a line that bisects the orbit transversely.
22/23	Orbitale	or	B	Most inferior point on the inferior orbital rim. Usually falls along the lateral half of the orbital margin.
24/25	Zygoorbitale	zo	B	Intersection of the orbital margin and the zygomaticomaxillary suture.
26/27	Maxillofrontale	mf	B	Intersection of the anterior lacrimal crest with the frontomaxillary suture.
28/29	Nasomaxillare	nm	B	Most inferior point of the nasomaxillary suture on the nasal aperture.
30/31	Alare	al	B	Instrumentally determined as the most lateral point on the nasal aperture in a transverse plan.
32/33	Piriform curvature	cp	B	Most infero-lateral point of the piriform aperture.
34/35	Nariale	na	B	Most inferior point of the piriform aperture.
36/37	Zygomaxillare	zm	B	Most inferior point on the zygomaticomaxillary suture.
38/39	Submaxillare curvature	csm	B	Most supero-medial point on the maxillary inflexion between the zygomaxillare and the ectomolar.
40/41	Supra canine	sc	B	Point on the superior alveolar ridge superior to the crown of the maxillary canine.

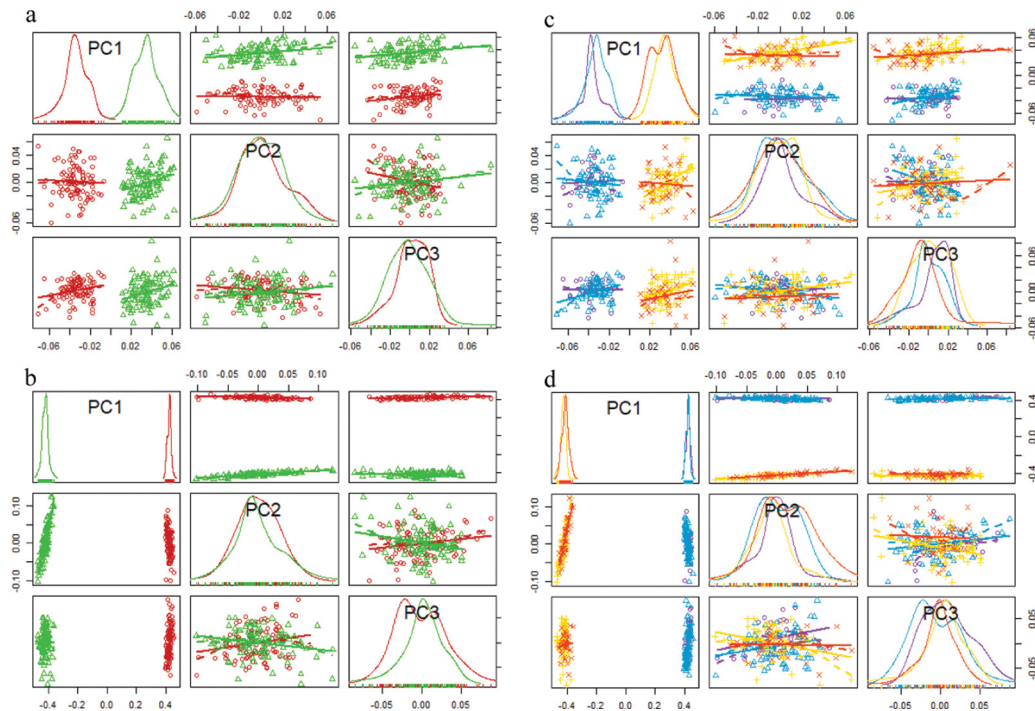


**Figure 2:** Between-group principal component (PC) analysis of external nasal soft tissue shape and mid-facial hard tissue and components grouped by population affinity (a,b) and by sex and population affinity (c,d). (a, c) Mid-facial hard tissue and (b, d) external nasal soft tissue. Red circles indicate black South Africans; green triangles indicate white South Africans; purple circles indicate black women; blue triangles indicate black men; yellow pluses indicate white women; and orange crosses indicate white men.

Geometric morphometric methods were used to quantify and evaluate shape differences attributable to population affinity, sex, size, age variables, and covariates in both shape configurations (soft and hard tissues). Geometric morphometrics reflects the geometry of the placed landmarks and enables visualisations of statistical findings as real shape deformations.<sup>23</sup>

Prior to statistical analysis, a general Procrustes analysis, a principal component analysis, and a multivariate normality test using Q-Q plots were run on both 3D reconstruction types for the complete sample and each population subgroup, namely white and black South Africans. First, a general Procrustes analysis was used to provide pose-invariant shape coordinates for both configurations.<sup>24,25</sup> Then, a principal component analysis was applied to minimise the dimensionality of the data and provide independent principal component scores that accounted for 95% of the sample's total variance. Finally, by evaluating Q-Q plots<sup>24</sup>, the normality of soft and hard tissue principal component scores was examined. The effect of the population affinity, sex, age, and allometry variables on the complete sample's soft and hard tissues was first performed. The expression of sexual dimorphism, ageing, and size effect (allometry) was then analysed for each subsample independently to identify population-specific variations. Finally, the covariations between nasal soft and hard tissue and population affinity dependency were analysed.

Using R-package geomorph<sup>26</sup>, simple and multiple analysis of variance (ANOVA/MANOVA) parametric tests were applied to examine shape variations across the population, sexes, and age groups. Additionally, R packages fmanova<sup>27</sup> and Morpho<sup>28</sup> were used to execute two non-parametric tests, 50-50 MANOVA<sup>27</sup> and permutation testing<sup>4</sup>, to support the findings. Finally, standard discriminant function analysis (DFA)<sup>4</sup> using the Morpho<sup>28</sup> R package was also carried out to categorise population affinity and sex based on leaving-one-out cross-validation to evaluate the classification's reliability.

Using the JVM R package<sup>29</sup>, allometry's impact was determined by generating linear models using soft and hard tissue configurations as response variables and population affinity, sex, age, and centroid size as predictors. The significance of each variable was determined

using 50-50 MANOVA and multivariate analysis of (co)variance (MANCOVA)<sup>29</sup> with Pillai trace. MANCOVA is employed to analyse the relationships between several dependent variables and one or more categorical or continuous explanatory factors.<sup>29</sup> In addition, the correlation between the two blocks of shape coordinates was examined using the two-block partial least squares<sup>30</sup> analysis available in the Geomorph R package.<sup>26</sup>

## Results

Multivariate normality analysis indicated non-parametric distributions for various hard tissue features, such as the anterior nasal aperture and the maxillary morphologies, for the complete sample and within population affinity subgroups. For this reason, all results were examined using both parametric and non-parametric tests, and outcomes were only judged acceptable if both tests yielded equivalent results. With regard to the intra- and inter-measurement errors of the craniometric (mean: 0.22 mm; SD: 0.02mm) and capulometric (mean: 0.23 mm; SD: 0.04 mm) landmark locations placed using the automatic landmarking procedure, lower mean values were found for both configurations (soft and hard tissues).

### Complete sample

The findings revealed that population affinity contributed the most to shape variance in the complete sample for both soft and hard tissue shape component configurations (Figure 2a,b). Moreover, all statistical tests (Table 2) demonstrated a significant difference between the population means. Finally, the classification reliability was 100% overall. (Table 2). Judging by visual observation in Figure 4a,b of the hard tissue (Figure 4a) and soft tissue (Figure 4c) mean shape representations, the wider shape could be attributed to black South Africans. The box plots (Figure 3a,b) further illustrated that the centroid sizes were slightly larger within black South Africans than in white South Africans. Nonetheless, this variance was limited in terms of the mean morphologies of the groups, showing relatively small shape variations related to population affinity specific size. Also, the interaction between size and population affinity testing reported non-significant differences for hard tissue, including all the skeletal elements evaluated separately, as well as for the soft tissue (Table 2).

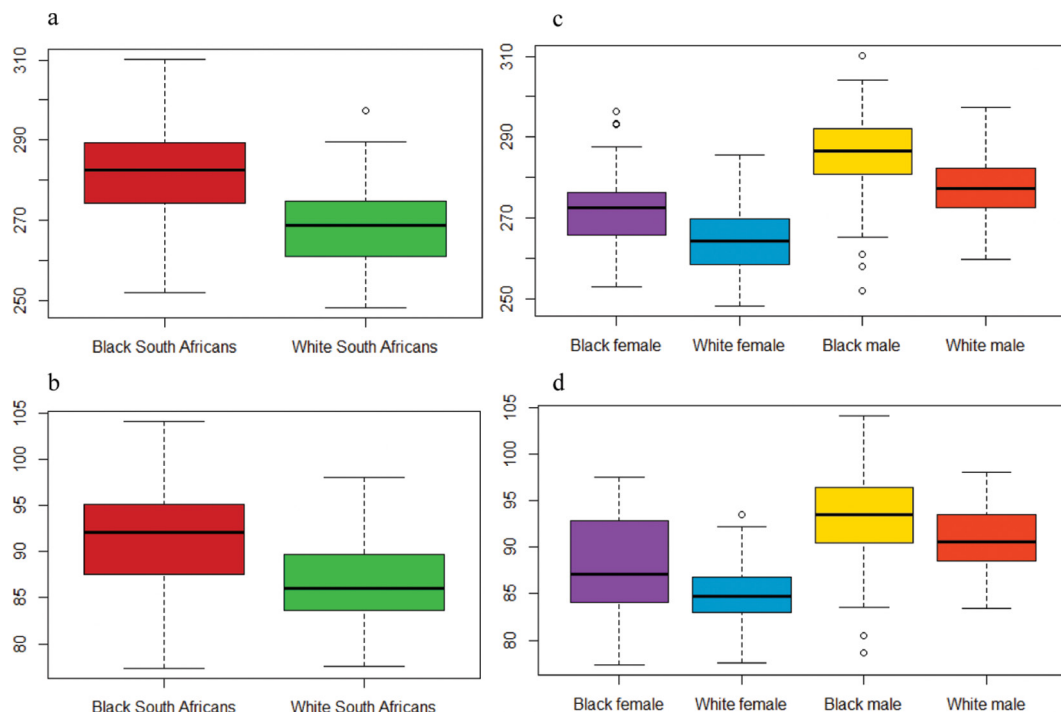


**Table 2:** Results of soft and hard tissue population affinity differences and covariation between soft and hard tissues and their dependence on population affinity

Complete sample	Population affinity				Black South African		White South Africans	
	Population affinity		Population affinity*Size		Covariation*		Covariation*	
	Test <sup>1</sup>	Test <sup>2</sup>	DFA	Test <sup>3</sup>	r-pls	p-value	r-pls	p-value
Mid-facial region	<b>0.001</b>	<b>0.001</b>	100%	0.431	0.613	<b>0.001</b>	0.563	<b>0.001</b>
Nasal bones	<b>0.001</b>	<b>0.001</b>	100%	0.216	0.562	<b>0.001</b>	0.545	<b>0.001</b>
Nasal bone (left)	<b>0.001</b>	<b>0.001</b>	99%	0.554	0.549	<b>0.001</b>	0.492	<b>0.002</b>
Nasal bone (right)	<b>0.001</b>	<b>0.001</b>	100%	0.583	0.584	<b>0.001</b>	0.515	<b>0.001</b>
Anterior nasal aperture	<b>0.001</b>	<b>0.001</b>	100%	0.623	0.468	<b>0.008</b>	0.523	<b>0.003</b>
Anterior nasal aperture (left)	<b>0.001</b>	<b>0.001</b>	99%	0.580	0.460	<b>0.007</b>	0.477	<b>0.008</b>
Anterior nasal aperture (right)	<b>0.001</b>	<b>0.001</b>	100%	0.563	0.467	<b>0.008</b>	0.468	<b>0.007</b>
Zygoma	<b>0.001</b>	<b>0.001</b>	100%	0.556	0.570	<b>0.001</b>	0.458	<b>0.022</b>
Zygomatic bone (left)	<b>0.001</b>	<b>0.001</b>	100%	0.553	0.536	<b>0.001</b>	0.465	<b>0.006</b>
Zygomatic bone (right)	<b>0.001</b>	<b>0.001</b>	100%	0.534	0.577	<b>0.001</b>	0.414	0.052
Maxilla	<b>0.001</b>	<b>0.001</b>	100%	0.598	0.605	<b>0.001</b>	0.540	<b>0.001</b>
Maxillary bone (left)	<b>0.001</b>	<b>0.001</b>	100%	0.627	0.587	<b>0.001</b>	0.518	<b>0.002</b>
Maxillary bone (right)	<b>0.001</b>	<b>0.001</b>	100%	0.623	0.570	<b>0.001</b>	0.330	0.505

Test<sup>1</sup>, MANOVA; Test<sup>2</sup>, permutation test; DFA, discriminant function analysis; Test<sup>3</sup>, ANOVA. Significant p-values (<0.05) are indicated in bold.

\*Correlation between mid-facial region and external nose tested by two-block partial least square (pls) analyses.


**Figure 3:** Centroid sizes grouped by population affinity (a,b) and by sex and population affinity (c,d) of the mid-facial hard tissue (a,c), and the external nasal soft tissue (b,d) shape components. Red: black South Africans; green: white South Africans; purple: black women; yellow: white women; blue: black men; orange: white men.

The external nose and the underlying mid-face configuration of the two South African populations appeared morphologically distinct (Figure 4a,b). Indeed, white South Africans were seen to have a longer and more prominent external nose than their black South African counterparts.

Furthermore, while evaluating the components of the mid-facial skeleton, the nasal bones of black South Africans appeared to be more integrated into the skull (or blunt), whereas the nasal bones were more prominent in white South Africans. The anterior nasal aperture of black South Africans

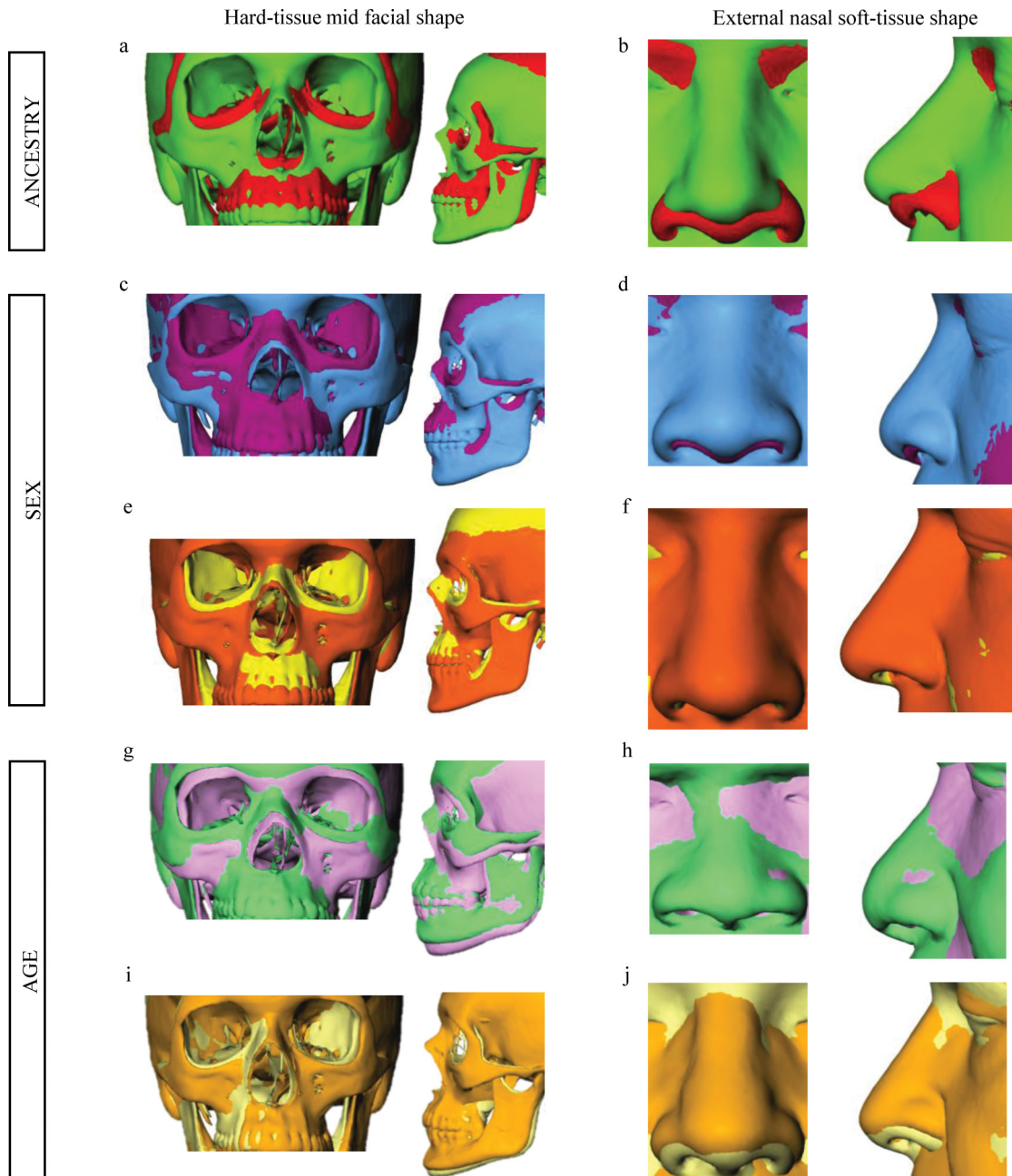


**Figure 4:** Mid-facial hard tissue and external nasal soft tissue shape differences between population affinity, sex, and age averages. (a,b) Mid-facial hard tissue and external nasal soft tissue shapes. Red: black South Africans; green: white South Africans. (c,d,e,f) Sexual dimorphism in mid-facial hard tissue and external nasal soft tissue shape differences for the black and white populations separately. (c,d) Soft and hard tissue shapes of black South Africans (purple: black women; blue: black men). (e,f) Soft and hard tissue shapes of white South Africans (yellow: white women; orange: white men). (g,h,i,j) Soft and hard tissue shape ageing differences for the black and white populations separately. (g,h) Soft and hard tissue shapes of black South Africans (purple: 18 years; green: 79 years). (i,j) Soft and hard tissue shapes of white South Africans (yellow: 18 years; orange: 79 years).

is wider and more rounded than that of white South Africans, which is smaller and more restricted (or pear-shaped). In terms of the maxilla, black South Africans displayed prognathism, while white South Africans displayed orthognathism. In both population groups, the zygomatic bones were retracted, although this was more pronounced in the white South Africans than in the black South Africans. Additionally, white South Africans have narrower zygomatic bones than black South Africans.

Sex interacted with population affinity in the complete soft and hard tissue sample. The between-group principal component analyses (Figure 2c,d) confirmed a strong separation between population groups and illustrated a similar expression with sexual dimorphism (Figure 4c,d,e,f) for both

soft (Figure 2c) and hard tissue (Figure 2d) shape components. However, when elements of the mid-facial shape were considered separately, the covariation between sex and population affinity was insignificant (Table 3), demonstrating the absence of population affinity specific expression of sexual dimorphism for the hard tissue shape. However, the interaction between sex and population affinity was statistically significant for the external nose, suggesting population affinity specific expression of sexual dimorphism (Table 3).

In the complete soft and hard tissue sample, the interaction of age and the covariate age with population affinity and sex was shown. For the underlying bone tissue morphology, all tests did not report a similar

**Table 3:** Soft and hard tissue sexual dimorphism in the complete sample and within population affinity groups

Complete sample	Black South Africans						White South Africans					
	Population affinity*Sex		Size*sex				Size*sex					
	Test <sup>4</sup>	Test <sup>5</sup>	Test <sup>1</sup>	Test <sup>2</sup>	Test <sup>4</sup>	DFA	Test <sup>3</sup>	Test <sup>1</sup>	Test <sup>2</sup>	Test <sup>4</sup>	DFA	Test <sup>3</sup>
Mid-facial region	0.325	0.253	<b>0.015</b>	<b>0.008</b>	<b>0.008</b>	96%	0.270	<b>0.017</b>	<b>0.019</b>	0.616	93%	0.501
Nasal bones	0.121	0.086	<b>0.053</b>	<b>0.049</b>	<b>0.000</b>	76%	0.631	0.158	0.164	<b>0.000</b>	83%	0.629
Nasal bone (left)	0.364	0.396	<b>0.036</b>	<b>0.034</b>	0.052	71%	0.619	0.068	<b>0.055</b>	0.014	70%	0.620
Nasal bone (right)	0.060	0.082	<b>0.006</b>	<b>0.006</b>	<b>0.000</b>	79%	0.558	0.165	0.178	<b>0.000</b>	80%	0.621
Anterior nasal aperture	0.622	0.562	<b>0.005</b>	<b>0.005</b>	<b>0.003</b>	82%	0.378	0.514	0.516	0.476	79%	0.152
Anterior nasal aperture (left)	0.400	0.097	<b>0.003</b>	<b>0.006</b>	<b>0.002</b>	82%	0.618	0.454	0.424	0.234	68%	0.615
Anterior nasal aperture (right)	0.555	0.495	<b>0.011</b>	<b>0.006</b>	<b>0.001</b>	76%	0.571	0.239	0.214	0.129	76%	0.587
Zygoma	0.249	0.372	<b>0.001</b>	<b>0.001</b>	<b>0.000</b>	91%	0.381	<b>0.001</b>	<b>0.001</b>	<b>0.000</b>	93%	0.593
Zygomatic bone (left)	0.394	0.502	<b>0.002</b>	<b>0.002</b>	<b>0.000</b>	86%	0.088	<b>0.001</b>	<b>0.001</b>	<b>0.000</b>	90%	0.532
Zygomatic bone (right)	0.684	0.765	<b>0.001</b>	<b>0.001</b>	<b>0.000</b>	84%	0.521	<b>0.002</b>	<b>0.001</b>	<b>0.000</b>	94%	0.516
Maxilla	0.397	0.311	<b>0.097</b>	0.107	<b>0.002</b>	88%	0.531	<b>0.029</b>	0.021	<b>0.000</b>	94%	0.579
Maxillary bone (left)	0.173	0.188	<b>0.025</b>	<b>0.032</b>	<b>0.000</b>	82%	0.684	<b>0.034</b>	0.025	<b>0.000</b>	90%	0.378
Maxillary bone (right)	0.275	0.228	0.133	0.147	<b>0.003</b>	82%	0.620	<b>0.013</b>	<b>0.008</b>	<b>0.000</b>	91%	0.641
External nose	<b>0.008</b>	<b>0.008</b>	<b>0.005</b>	<b>0.005</b>	<b>0.014</b>	88%	0.679	<b>0.001</b>	<b>0.001</b>	<b>0.016</b>	90%	0.378

Test<sup>1</sup>, MANOVA; Test<sup>2</sup>, Permutation test; Test<sup>3</sup>, ANOVA; Test<sup>4</sup>, MANCOVA; Test<sup>5</sup>, 50-50 MANOVA; DFA, discriminant function analysis. Significant p-values (<0.05) are indicated in bold.

outcome for age, but significance was reported for the covariation between population affinity and age (Table 4). Regarding the soft tissue shape, both parametric and non-parametric tests reported significance with age, and for the interaction between age and population affinity. When the hard tissue elements were analysed separately, the right anterior nasal aperture and the right maxilla seemed to show a higher variability of shape with ageing when compared to the other skeletal elements, as well as for the interaction between population affinity and age (Table 4). On the other hand, apart from the right maxillary bone, all tests on soft tissue and skeletal elements reported significance for the interaction between sex and age, or for the interaction among population affinity, sex, and age. Age and its interaction with population affinity significantly contributed to overall soft and hard tissue shape variation (Figure 4g,h,i,j).

All three variables – population affinity, sex, and centroid size – were examined to create an impression of the extent to which allometry is responsible for variability in the morphology of soft and hard tissues in the complete sample. All statistical tests indicated size significance for the hard tissue shape (Table 5). In addition, the nasal bones, the left anterior nasal aperture, the left zygomatic bone, and the left maxillary bone were significant for the interaction between size and population affinity when all parts of the hard tissue area were evaluated independently. On the other hand, no significance was found for the interaction between sex and size, and only the nasal aperture and the maxilla showed a significant interaction among population affinity, sex, and size, with both parametric and non-parametric tests. Regarding the soft tissue shape, both parametric and non-parametric statistical tests reported significance for size (Table 5). No significant interaction was observed between population affinity and size, or among population affinity, sex, and size for soft tissue shapes. Overall, size is an essential contributor to the variation found in the soft and hard tissue shapes.

### Population affinity subsamples

Population affinity differences were visible within the data, and to identify significant population affinity specific variations, the expression of sexual

dimorphism, the ageing process, and the impact of size (allometry) were analysed for each population affinity subsample (white and black subsamples) separately and on both soft and hard tissues.

Sexual dimorphism was verified in all hard tissue elements in the black South African sample (Table 3), while only the maxillary and the right maxillary shapes had no significance in parametric and non-parametric tests. For the hard tissue structure, a DFA showed an accuracy rate of 96%. When we examined the anatomical parts independently in the black South African population, the zygomatic morphology showed the most significant sexual dimorphism, with a DFA of 91%. Only the morphology of the zygoma and the maxilla demonstrated the presence of sexual dimorphism in the white South African population, with DFA achieving 93% and 94% accuracy, respectively. Sexual dimorphism in the soft tissue shape was confirmed in both populations (Table 3). Although sexual dimorphism of the soft tissue shape was accentuated for the white South African sample, all tests also reported significant differences between group means for the black South African sample. A DFA on the soft tissue shape revealed an accuracy of 88% for the black South African sample and 90% for the white South African group, demonstrating the prevalence of sexual dimorphism in both populations.

The soft tissue and hard tissue shape differences between sex averages for black South Africans (Figure 4c,d) and white South Africans (Figure 4e,f) confirm the statistical findings of sexual dimorphism in each population group. Non-significant differences in the size variations for the hard tissue, including all the skeletal elements evaluated separately, as well as for the soft tissue (Table 3), were noted. For both population affinity groups and for both soft and hard tissue shape configurations, the centroid sizes were slightly larger in the male individuals than in the female individuals (Figure 3c,d), demonstrating that the expression of sexual dimorphism regarding centroid size is therefore very similar in each population group.

Table 5 shows that, in both groups, age had a statistically significant influence on hard tissue morphology, demonstrating that age affects hard tissue shape variation. There was a strong correlation between

**Table 4:** Soft and hard tissue shape change associated with age in the complete sample and within population affinity groups

	Complete sample								Black South Africans				White South Africans			
	Age		Population affinity* Age		Sex*Age		Population affinity*Sex* Age		Age		Sex*Age		Age		Sex*Age	
	Test <sup>4</sup>	Test <sup>5</sup>	Test <sup>4</sup>	Test <sup>5</sup>	Test <sup>4</sup>	Test <sup>5</sup>	Test <sup>4</sup>	Test <sup>5</sup>	Test <sup>4</sup>	Test <sup>5</sup>	Test <sup>4</sup>	Test <sup>5</sup>	Test <sup>4</sup>	Test <sup>5</sup>	Test <sup>4</sup>	Test <sup>5</sup>
Mid-facial region	0.054	<b>0.012</b>	<b>0.002</b>	<b>0.000</b>	<b>0.454</b>	0.288	0.317	0.302	<b>0.006</b>	<b>0.000</b>	<b>0.001</b>	0.064	<b>0.001</b>	<b>0.015</b>	<b>0.020</b>	<b>0.015</b>
Nasal bones	0.420	0.309	0.763	0.484	0.501	0.760	0.989	0.996	0.357	0.372	0.880	0.863	0.401	0.429	0.306	0.328
Nasal bone (left)	0.363	0.230	0.740	0.547	0.782	0.632	0.931	0.975	0.670	0.694	0.758	0.770	0.548	0.583	0.565	0.586
Nasal bone (right)	0.507	0.298	0.391	0.266	0.302	0.412	0.981	0.952	0.595	0.581	0.770	0.775	0.548	0.548	0.754	0.797
Anterior nasal aperture	0.109	0.127	<b>0.017</b>	<b>0.003</b>	0.746	0.842	0.687	0.691	<b>0.009</b>	<b>0.000</b>	<b>0.008</b>	0.057	0.134	<b>0.038</b>	0.826	0.901
Anterior nasal aperture (left)	0.112	<b>0.032</b>	<b>0.034</b>	<b>0.011</b>	0.598	0.796	0.348	0.533	0.115	<b>0.057</b>	0.368	<b>0.454</b>	0.282	0.276	0.904	0.934
Anterior nasal aperture (right)	<b>0.024</b>	<b>0.036</b>	0.134	0.108	0.433	0.625	0.081	0.052	<b>0.011</b>	<b>0.002</b>	<b>0.003</b>	<b>0.002</b>	0.080	<b>0.030</b>	0.748	0.731
Zygoma	0.530	0.596	<b>0.014</b>	0.145	0.896	0.791	0.769	0.700	<b>0.040</b>	0.092	0.070	0.151	0.102	0.079	0.521	0.412
Zygomatic bone (left)	0.373	0.450	<b>0.038</b>	0.165	0.737	0.674	0.210	0.193	0.121	0.113	0.153	0.155	0.574	0.408	0.304	0.188
Zygomatic bone (right)	0.190	0.302	<b>0.026</b>	0.060	0.518	0.467	0.151	0.098	<b>0.042</b>	<b>0.023</b>	0.098	<b>0.030</b>	0.159	0.078	0.732	0.518
Maxilla	0.132	0.064	<b>0.015</b>	<b>0.000</b>	0.228	0.370	0.129	0.117	0.149	<b>0.001</b>	0.280	<b>0.028</b>	0.031	0.090	0.119	0.121
Maxillary bone (left)	0.137	0.094	<b>0.079</b>	<b>0.038</b>	0.379	0.279	0.587	0.528	<b>0.016</b>	<b>0.011</b>	0.679	0.720	0.185	0.393	0.566	0.376
Maxillary bone (right)	<b>0.004</b>	<b>0.001</b>	0.101	<b>0.019</b>	<b>0.009</b>	0.020	0.005	<b>0.002</b>	0.109	<b>0.043</b>	<b>0.044</b>	<b>0.046</b>	<b>0.039</b>	0.057	0.075	<b>0.017</b>
External nose	<b>0.001</b>	<b>0.000</b>	<b>0.009</b>	<b>0.010</b>	0.674	0.665	0.723	0.730	<b>0.000</b>	<b>0.000</b>	<b>0.002</b>	0.595	<b>0.007</b>	<b>0.006</b>	0.754	0.876

Test<sup>4</sup>, MANCOVA; Test<sup>5</sup>, 50-50 MANOVA. Significant p-values (<0.05) are indicated in bold.

the form of the anterior nasal aperture, right zygoma and left maxilla in the black South African sample and the impact of age on shape variability in the white South African sample, according to all statistical tests. In both samples, significant interactions between age and sex were found in the hard tissue shape, indicating that sex-dependent ageing processes exist. In addition, all tests reported a significant influence of age on the soft tissue, suggesting that age affects, or at least influences, shape variability of the external nose (Table 4) in both population groups. No significance was found for the interaction of sex and age on the soft tissue, indicating that the influence of ageing was independent of sex.

The statistical findings on ageing processes in each group are confirmed in Figure 4, representing the external nose and the underlying hard tissue shape differences between average age from 18 to 79 years for black South Africans (Figure 4g,h) and white South Africans (Figure 4i,j).

Separately for both population affinity groups, all tests showed significance for size for all soft and hard tissue components. In both groups, no statistical significance was noted for the interaction between

sex and size on the soft and hard tissue shapes, demonstrating a similar trend for allometry between the sexes and tissue types. Only the left zygomatic bone and the right maxillary bone showed a significant interaction between sex and size in the black South African sample (Table 5). In both population groups, size is essential for explaining soft and hard tissue shape variability.

### **Covariation within soft and hard tissues in each population affinity subsample**

Population affinity is paramount to evaluating shape variation in the soft and hard tissues of the nose. Therefore, to assess covariation within soft and hard tissue morphology and its reliance upon population affinity, the data set was divided into subgroups specific to ethnicity (white South African and black South African). In black South Africans, all correlations between soft and hard tissue components were reported to be significant. In comparison, most variables, excluding zygomatic matrices and the right maxillary component, were significantly correlated within white South Africans (Table 2).



**Table 5:** Soft and hard tissue shape changes associated with size in the complete sample and within population affinity groups

Complete sample									Black South Africans				White South Africans			
	Size		Population affinity*Size		Sex*Size		Population affinity*Sex*Size		Size		Sex*Size		Size		Sex*Size	
	Test <sup>4</sup>	Test <sup>5</sup>	Test <sup>4</sup>	Test <sup>5</sup>	Test <sup>4</sup>	Test <sup>5</sup>	Test <sup>4</sup>	Test <sup>5</sup>	Test <sup>4</sup>	Test <sup>5</sup>	Test <sup>4</sup>	Test <sup>5</sup>	Test <sup>4</sup>	Test <sup>5</sup>	Test <sup>4</sup>	Test <sup>5</sup>
Mid-facial region	<b>0.000</b>	<b>0.000</b>	0.527	0.478	0.636	0.728	0.467	0.716	<b>0.000</b>	<b>0.000</b>	0.280	0.277	<b>0.000</b>	<b>0.000</b>	0.124	0.098
Nasal bones	<b>0.000</b>	<b>0.000</b>	<b>0.000</b>	<b>0.002</b>	0.611	0.445	0.313	0.238	<b>0.000</b>	<b>0.000</b>	0.229	0.190	<b>0.000</b>	<b>0.000</b>	0.718	0.676
Nasal bone (left)	<b>0.000</b>	<b>0.000</b>	<b>0.000</b>	0.144	0.312	0.248	0.577	0.476	<b>0.000</b>	<b>0.000</b>	0.142	0.142	<b>0.000</b>	<b>0.000</b>	0.780	0.780
Nasal bone (right)	<b>0.000</b>	<b>0.000</b>	<b>0.014</b>	<b>0.004</b>	0.287	0.208	0.466	0.658	<b>0.000</b>	<b>0.000</b>	0.323	0.324	<b>0.000</b>	<b>0.000</b>	0.632	0.632
Anterior nasal aperture	<b>0.000</b>	<b>0.000</b>	0.263	0.215	0.559	0.444	<b>0.023</b>	<b>0.013</b>	<b>0.000</b>	<b>0.000</b>	0.462	0.406	<b>0.000</b>	<b>0.000</b>	0.090	0.072
Anterior nasal aperture (left)	<b>0.000</b>	<b>0.000</b>	<b>0.000</b>	<b>0.021</b>	<b>0.029</b>	0.122	0.355	0.092	<b>0.000</b>	<b>0.000</b>	0.042	0.065	<b>0.000</b>	<b>0.000</b>	0.135	0.135
Anterior nasal aperture (right)	<b>0.000</b>	<b>0.000</b>	0.460	0.329	0.135	<b>0.099</b>	0.159	0.137	<b>0.000</b>	<b>0.000</b>	0.690	0.629	<b>0.000</b>	<b>0.000</b>	0.106	0.085
Zygoma	<b>0.000</b>	<b>0.000</b>	0.227	0.166	0.405	0.357	0.264	0.212	<b>0.000</b>	<b>0.000</b>	0.125	0.187	<b>0.000</b>	<b>0.000</b>	0.122	0.362
Zygomatic bone (left)	<b>0.000</b>	<b>0.000</b>	<b>0.017</b>	<b>0.010</b>	0.298	0.337	0.552	0.487	<b>0.000</b>	<b>0.000</b>	<b>0.044</b>	<b>0.029</b>	<b>0.000</b>	<b>0.000</b>	0.230	0.375
Zygomatic bone (right)	<b>0.000</b>	<b>0.000</b>	0.149	0.078	0.561	0.482	0.380	0.481	<b>0.000</b>	<b>0.000</b>	0.373	0.558	<b>0.000</b>	<b>0.000</b>	0.856	0.984
Maxilla	<b>0.000</b>	<b>0.000</b>	0.074	<b>0.044</b>	0.718	0.655	<b>0.005</b>	<b>0.012</b>	<b>0.000</b>	<b>0.000</b>	0.135	0.303	<b>0.000</b>	<b>0.000</b>	0.780	0.709
Maxillary bone (left)	<b>0.000</b>	<b>0.000</b>	<b>0.024</b>	<b>0.013</b>	0.911	0.856	0.162	0.127	<b>0.000</b>	<b>0.000</b>	0.829	0.749	<b>0.000</b>	<b>0.000</b>	0.532	0.473
Maxillary bone (right)	<b>0.000</b>	<b>0.000</b>	<b>0.012</b>	<b>0.085</b>	0.610	0.593	<b>0.000</b>	<b>0.000</b>	<b>0.002</b>	<b>0.001</b>	<b>0.006</b>	<b>0.003</b>	<b>0.000</b>	<b>0.000</b>	0.577	0.515
External nose	<b>0.000</b>	<b>0.000</b>	0.167	0.189	0.932	0.932	0.383	0.383	<b>0.000</b>	<b>0.000</b>	0.138	0.191	0.809	<b>0.000</b>	<b>0.047</b>	0.530

Test<sup>4</sup>, MANCOVA; Test<sup>5</sup>, 50-50 MANOVA. Significant *p*-values (<0.05) are indicated in bold.

## Discussion

Variation in the mid-facial skeleton and related soft tissue (the external nose) is influenced by a variety of factors, including population affinity, sex, age and allometry. Nasal shape variation results from the divergent development and growth of the craniofacial skeleton. This biological variation, in both soft and hard tissues, can be attributed to hormonal, genetic and epigenetic factors as well as external stimuli (e.g. biomechanical factors)<sup>31-34</sup> and must be considered in the approximation of the nose. The understanding and quantification of human biological phenotypes allow for the development of accurate facial approximation guidelines applicable to forensic anthropology.

During skeletal development, and to preserve function and proportionate growth, the bony elements of the face fluctuate in size and morphology, as well as in location within the craniofacial complex.<sup>31-33</sup> During growth, the skull evolves through two concurrent and inter-associated processes, namely 'modelling' and 'displacements' of the skeletal components.<sup>31-33</sup> Due to the bone growth biomechanics of craniofacial morphology, such as the resorption of the canine fossae, the nasal area, and the inferior edge of the zygomatic region, the adult face exhibits forward and downward development directions.<sup>34</sup> During adulthood, the remodelling of the underlying skeletal structure<sup>34</sup> and changes in the facial musculature resulting from gravity and the effects of hyperdynamic facial expressions may influence the soft tissue morphology of the nose with advancing ageing.<sup>34</sup> Literature indicates that facial soft tissue ageing varies by a decade of life, gender, and population affinity.<sup>34</sup> Consequently, our findings demonstrate that the remodelling of the underlying skeletal structure influences the shape of the nose throughout craniofacial development, highlighting that the

components of the nose cannot be regarded as independent aspects of the craniofacial skeleton and that the effect of variables such as population affinity, sex, and age must be taken into account to interpret the observed variation.

Several bio-anthropological studies have demonstrated the effect of environmental variables on variance in nose morphology across populations.<sup>10</sup> Generally, researchers consider that the shape of the external nose and the anterior nasal aperture contribute to climate adaptation by controlling air temperature to protect the pulmonary functions against extreme environments.<sup>10</sup> On account of geographical variation, physical anthropologists are able to estimate population affinity by translating biological traits to a culturally elaborated labelling system.<sup>35</sup>

In addition, Serre and Pääbo<sup>36</sup> noted a close relationship between biology and culture and stated that "genetic discontinuities seen between population groups are not racial or continental in nature but depend on historical and cultural factors". Moreover, Ousley and colleagues<sup>6</sup> have demonstrated that biological phenotypic variation within population groups is quantifiable and may be useful in providing a potential classification of an unknown individual. Morphological variation is observed over geographical distances, which is often driven by cultural and social aptitudes.<sup>9</sup>

Apartheid-era categories are no longer enforced by law in South Africa; yet contemporary South Africans continue to self-identify according to such classifications. People's cultural position in the nation depends on their ability to socially identify as a member of one of the several South African ethnicities.<sup>37</sup> As a result, the majority of South Africans (80.5%) identify as black, followed by coloured (8.8%),

white (8.3%), and Indian/Asian (2.5%).<sup>37</sup> The assortative mating within these groups has bolstered the already evident morphological differences within and across groups<sup>20</sup>, resulting in the continuation of skeletal variation.<sup>20</sup> Consequently, the three primary social categories of South Africans are now black, coloured and white.

Several studies have described distinct biological variations in mid-facial shape and size among South African groups.<sup>11-13,38</sup> Indeed, distinct characteristics from the mid-face, such as inter-orbital breadth, nasal width, alveolar prognathism and nasal bone morphology, are significant population affinity related phenotypic variations.<sup>11-13,38</sup> Variation in nasal soft and hard tissue structures between and among worldwide population groups has also been described.<sup>4</sup> For instance, Schlager<sup>4</sup> observed a significant difference in soft and hard tissue nasal morphologies between Chinese and European groups. While European nasal features are relatively pronounced, Chinese nasal shapes are smoother and more integrated into the craniofacial skeleton.<sup>4</sup> In our study, black and white South Africans demonstrated distinct population shape variation in soft and hard tissues. These variations present a challenge for facial reconstruction. Few effective techniques exist that take into account the influences of biological parameters (population affinity, sex, age) on the morphology of the face.<sup>4,38</sup> Current facial approximation approaches restrict the objectivity and precision of the reconstruction by ignoring population-specific variables. Recent research among South African groups<sup>39</sup> and on other European and Asian populations<sup>4</sup> emphasises the significance of taking into account the effect of variables such as population affinity, sex, and age on the approximation of the nose. Disregarding biological parameters when initiating approximations will affect the precision of the final facial reconstruction.

The assessment of sex is dependent on quantifying and interpreting the manifestation of sexual dimorphism in a population.<sup>40,41</sup> Based on our results, sexual dimorphism plays a crucial role in the overall variance of the nose's soft and hard tissues and might help discriminate between the sexes. At birth, babies display a slight sexual dimorphism, with significant divergence occurring during puberty, which is also expressed as variation in nasal dimensions.<sup>42</sup> In recent literature, variation in nasal complex shape has been investigated using standard morphometric methods, based on angles and distances<sup>43-46</sup> or soft tissue thickness<sup>43</sup>, that address a link between asymmetry and facial masculinity.

In CFR, the nose is crucial in differentiating female and male facial features, and therefore contributes to the creation of precise facial approximation of an unknown individual.<sup>46</sup>

Only one approach, developed by Schlager<sup>4</sup> using GMM on Chinese and European samples, has been used to address these challenges for reconstructing the nose. Schlager<sup>4</sup> observed that population affinity seemed to statistically impact the manifestation of sexual dimorphism in differences in the shape of the nose among Chinese and European populations. Nevertheless, Schlager emphasised that "this impact is negligible from a biological standpoint". Numerous studies<sup>8,11-13</sup> using conventional morphometric techniques have shown considerable variation in facial skeletal morphology (size and form) between the sexes in the South African research environment. In general, it has been established that sexual dimorphism is less pronounced in the black South African population than in other populations (white and coloured).<sup>8,11-13</sup>

In our study, visualisations of sexual dimorphism suggest that the shape change is consistent between soft and hard tissue configurations, and that the general similarity seems to outweigh the difference. Nonetheless, the sex distribution in each sample (100 black South Africans (33 female, 67 male) and 100 white South Africans (65 female, 35 male)) may affect the findings on sexual dimorphism to some extent.

Ageing is almost as important as sex when considering variation in both soft and hard tissue shapes. Generally, studies focus on standard metric measurements<sup>44,45</sup> and/or additional area and volume analyses<sup>44</sup>

of the external nose. These studies have revealed ageing-related nose lengthening, broadening, and angle changes.<sup>44,45</sup>

Few studies using GMM describe age-related craniofacial shape variations. Only two recent findings, on a French sample<sup>46</sup> and a Chinese and European sample<sup>4</sup>, found age-related changes in adults' external nose dimensions.

Our results on age-induced changes in the shape of soft tissues are similar to those of prior research using conventional anthropometric techniques. Indeed, in both population affinity groups, age influenced soft and hard tissue shape. In this research, we observed that age-related morphological differences across population affinity might be explained by tissue deterioration and the effects of gravity. However, findings on the effect of ageing may, to some extent, be impacted by the sample's age distribution.

## Conclusion

Population affinity, sex, age, and size (allometry) influence the biological variability of the nasal complex, both in soft and hard tissue shapes. Population affinity was found to be an essential factor for shape variation within the sample, highlighting population affinity specific differences. Additionally, within population affinity groups, sexual dimorphism and ageing appeared to influence distinct elements of the shape of the mid-facial region. From the findings, the two South African groups varied considerably in terms of soft- and hard-tissue nasal complex shapes and their correlations, emphasising the importance of considering biological parameters and highlighting the need for population-specific, accurate, and reliable 3D statistical prediction methods. The current situation of unidentified persons in South Africa will significantly benefit from research into morphological variation among modern South African populations to generate consistent and precise identification guidelines, such as using South African standard facial reconstruction methods.

## Acknowledgements

We thank Dr André Uys from the Oral and Dental Hospital, University of Pretoria, South Africa, and Dr Sarel Botha from the Life Groenkloof Hospital, Pretoria, South Africa, for providing the CBCT data. We acknowledge the AESOP+ consortia coordinated by Prof. José Braga (Université Paul-Sabatier, Toulouse, France/ University of the Witwatersrand, Johannesburg, South Africa), and the Erasmus Mundus programme, Bakeng se Afrika, coordinated by Prof. Ericka L'Abbé (University of Pretoria, Pretoria, South Africa) and Prof. Anna Oettlé (Sefako Makgatho Health Sciences University, Ga-Rankuwa, Pretoria, South Africa).

## Competing interests

We have no competing interests to declare.

## Authors' contributions

A.F.R.: Conceptualisation, methodology, data collection, data analysis, validation, data curation; writing – the initial draft, writing – revisions, project leadership, funding acquisition. F.D.: Validation, writing – revisions. E.N.L.: Conceptualisation, validation, writing – revisions, student supervision, project leadership. D.V.: Conceptualisation, methodology, data analysis, validation, writing – revisions, project leadership. A.C.O.: Conceptualisation, writing – revisions, student supervision, project leadership, project management.

## References

1. White JD, Ortega-Castrillón A, Matthews H, Zaidi AA, Ekrami O, Snyders J, et al. MeshMonk: Open-source large-scale intensive 3D phenotyping. *Sci Rep.* 2019;9, Art. #6085. <https://doi.org/10.1038/s41598-019-42533-y>
2. Baillie LJ, Muirhead JC, Blyth P, Niven BE, Dias GJ. Position effect on facial soft tissue depths: A sonographic investigation. *J Forensic Sci.* 2016;61:S60–S70. <https://doi.org/10.1111/1556-4029.12935>



3. Sipahioğlu S, Ulubay H, Diren HB. Midline facial soft tissue thickness database of Turkish population: MRI study. *Forensic Sci Int.* 2012;219:282.e1–282.e8. <https://doi.org/10.1016/j.forsciint.2011.11.017>
4. Schlager S. Soft-tissue reconstruction of the human nose: Population differences and sexual dimorphism [dissertation]. Freiburg: Albert Ludwig University of Freiburg; 2013.
5. Ridet A, Demeter F, Galland M, L'abbé E, Vandermeulen D, Oettlé A. Automatic landmarking as a convenient prerequisite for geometric morphometrics. Validation on cone beam computed tomography (CBCT)-based shape analysis of the nasal complex. *Forensic Sci Int.* 2020;306, Art. #110095. <https://doi.org/10.1016/j.forsciint.2019.110095>
6. Ousley S, Jantz R, Freid D. Understanding race and human variation: Why forensic anthropologists are good at identifying race. *Am J Phys Anthropol.* 2009;139:68–76. <https://doi.org/10.1002/ajpa.21006>
7. Fagertun J, Harder S, Rosengren A, Moeller C, Werge T, Paulsen RR, et al. 3D facial landmarks: Inter-operator variability of manual annotation. *BMC Med Imaging.* 2014;14:35. <https://doi.org/10.1186/1471-2342-14-35>
8. Ridet AF, Demeter F, L'abbé EN, Vandermeulen D, Oettlé AC. Nose approximation among South African groups from cone-beam computed tomography (CBCT) using a new computer-assisted method based on automatic landmarking. *Forensic Sci Int.* 2020;313, Art. #110357. <https://doi.org/10.1016/j.forsciint.2020.110357>
9. L'Abbé EN, Kenyhercz M, Stull KE, Ousley SD. Craniometric assessment of modern 20th century black, white and coloured South Africans. In: *Proceedings of the 65<sup>th</sup> Annual Meeting of the American Academy of Forensic Sciences*; 2013 February; Washington DC, USA. Colorado Springs, CO: AAFS; 2013. p. 444. Available from: [https://www.aafs.org/sites/default/files/media/documents/2013\\_Proceedings.pdf](https://www.aafs.org/sites/default/files/media/documents/2013_Proceedings.pdf)
10. Franciscus RG, Long JC. Variation in human nasal height and breadth. *Am J Phys Anthropol.* 1991;85:419–427. <https://doi.org/10.1002/ajpa.1330850406>
11. L'Abbé EN, Van Rooyen C, Nawrocki SP, Becker PJ. An evaluation of non-metric cranial traits used to estimate ancestry in a South African sample. *Forensic Sci Int.* 2011;209:195.e1–195.e7. <https://doi.org/10.1016/j.forsciint.2011.04.002>
12. McDowell JL, L'Abbé EN, Kenyhercz MW. Nasal aperture shape evaluation between black and white South Africans. *Forensic Sci Int.* 2012;222:397.e1–397.e6. <https://doi.org/10.1016/j.forsciint.2012.06.007>
13. McDowell JL, Kenyhercz MW, L'Abbé EN. An evaluation of nasal bone and aperture shape among three South African populations. *Forensic Sci Int.* 2015;252:189.e1–189.e7. <https://doi.org/10.1016/j.forsciint.2015.04.016>
14. L'Abbé EN, Loots M, Meiring JH. The Pretoria bone collection: A modern South African skeletal sample. *HOMO.* 2005;56:197–205. <https://doi.org/10.1016/j.jchb.2004.10.004>
15. Tyrrell AJ, Evison MP, Chamberlain AT, Green MA. Forensic three-dimensional facial reconstruction: Historical review and contemporary developments. *J Forensic Sci.* 1997;42:653–661. <https://doi.org/10.1520/JFS14176J>
16. Vandermeulen D, Claes P, De Greef S, Willems G, Clement J, Suetens P. Automated facial reconstruction. In: Wilkinson C, Rynn C, editors. *Craniofacial identification*. Cambridge: Cambridge University Press; 2012. p. 203. <https://doi.org/10.1017/CBO9781139049566.017>
17. Claes P, Vandermeulen D, De Greef S, Willems G, Clement JG, Suetens P. Computerized craniofacial reconstruction: Conceptual framework and review. *Forensic Sci Int.* 2010;201:138–145. <https://doi.org/10.1016/j.forsciint.2010.03.008>
18. Krüger GC, Liebenberg L, Myburgh J, Meyer A, Oettlé AC, Botha D, et al. Forensic anthropology and the biological profile in South Africa. In: Latham KE, Bartelink EJ, Finnegan M, editors. *New perspectives in forensic human skeletal identification*. Cambridge: Academic Press; 2018. p. 313–321. <https://doi.org/10.1016/B978-0-12-805429-1.00027-2>
19. Franklin D, Freedman L, Milne N, Oxnard CE. Geometric morphometric study of population variation in indigenous Southern African crania. *Am J Hum Biol.* 2007;19:20–33. <https://doi.org/10.1002/ajhb.20569>
20. Sutherland C. Biological distance among modern and parental South African groups using discrete traits of the skull [MSc dissertation]. Pretoria: University of Pretoria; 2016.
21. Cople J, Stephan CN. A standardized nomenclature for craniofacial and facial anthropometry. *Int J Legal Med.* 2016;130:863–879. <https://doi.org/10.1007/s00414-015-1292-1>
22. R. The R Project for statistical computing [cited 2020 May 12]. Indianapolis, IN: The R Foundation; n.d. Available from: <https://www.r-project.org/>
23. Bookstein FL. Shape and the information in medical images: A decade of the morphometric synthesis. *CVIU.* 1997;66:97–118. <https://doi.org/10.1006/cviu.1997.0607>
24. Balakrishnan N, Colton T, Everitt B, Piegorsch W, Ruggeri F, Teugels JL, editors. *Wiley StatsRef: Statistics Reference Online*. Hoboken, NJ: Wiley; 2014. <https://doi.org/10.1002/9781118445112>
25. Slice DE. Landmark coordinates aligned by Procrustes analysis do not lie in Kendall's shape space. *Syst Biol.* 2001;50:141–149. <https://doi.org/10.1080/10635150119119110>
26. Adams D, Collyer M, Kaliontzopoulou A, Baken E. Geometric morphometric analyses of 2D/3D landmark data. *geomorphR/geomorph*. R Foundation; 2024. Available from: <https://cran.r-project.org/web/packages/geomorph/index.html>
27. Langsrud Ø. 50-50 multivariate analysis of variance for collinear responses. *J R Statist Soc D.* 2002;51:305–317. <https://doi.org/10.1111/1467-9884.00320>
28. Schlager S. *zarquon42b/Morpho* [software on the Internet]. Available from: <https://github.com/zarquon42b/Morpho>.
29. Selker R, Love J, Dropmann D, Moreno V. The 'jamovi' analyses [software on the Internet]. Available from: <https://cran.r-project.org/web/packages/jm/index.html>
30. Rohlf FJ, Corti M. Use of two-block partial least-squares to study covariation in shape. *Syst Biol.* 2000;49:740–753. <https://doi.org/10.1080/106351500750049806>
31. Atchley WR, Hall BK. A model for development and evolution of complex morphological structures. *Biol Rev.* 1991;66:101–157. <https://doi.org/10.1111/j.1469-185X.1991.tb01138.x>
32. Lieberman D. *The evolution of the human head*. Cambridge, MA: Belknap Press of Harvard University Press; 2011.
33. Bastir M. A systems-model for the morphological analysis of integration and modularity in human craniofacial evolution. *J Anthropol Sci.* 2008;86:37–58.
34. Albert AM, Ricaneck K, Patterson E. A review of the literature on the aging adult skull and face: Implications for forensic science research and applications. *Forensic Sci Int.* 2007;172:1–9. <https://doi.org/10.1016/j.forsciint.2007.03.015>
35. Sauer NJ. Forensic anthropology and the concept of race: If races don't exist, why are forensic anthropologists so good at identifying them? *Soc Sci Med.* 1992;34:107–111. [https://doi.org/10.1016/0277-9536\(92\)90086-6](https://doi.org/10.1016/0277-9536(92)90086-6)
36. Serre D, Pääbo S. Evidence for gradients of human genetic diversity within and among continents. *Genome Res.* 2004;14:1679–1685. <https://doi.org/10.1101/gr.2529604>
37. Statistics South Africa (Stats SA). Mid-year population estimates (census no. P0302). Pretoria: Stats SA; 2015.
38. Oettlé AC, Demeter FP, L'abbé EN. Ancestral variations in the shape and size of the zygoma: Ancestral variations of the zygoma. *Anat Rec.* 2017;300:196–208. <https://doi.org/10.1002/ar.23469>
39. Ridet AF, Demeter F, Liebenberg J, L'Abbé EN, Vandermeulen D, Oettlé AC. Skeletal dimensions as predictors for the shape of the nose in a South African sample: A cone-beam computed tomography (CBCT) study. *Forensic Sci Int.* 2018;289:18–26. <https://doi.org/10.1016/j.forsciint.2018.05.011>
40. Gapert R, Black S, Last J. Sex determination from the occipital condyle: Discriminant function analysis in an eighteenth and nineteenth century British sample. *Am J Phys Anthropol.* 2009;138:384–394. <https://doi.org/10.1002/ajpa.20946>
41. Chronicle EP, Chan M-Y, Hawkings C, Mason K, Smethurst K, Stallybrass K, et al. You can tell by the nose—judging sex from an isolated facial feature. *Perception.* 1995;24:969–973. <https://doi.org/10.1068/p240969>



42. Troncoso Pazos JA, Suazo Galdames IC, Cantín López M, Zavando Matamata DA. Sexual dimorphism in the nose morphotype in adult Chilean. *Int J Morphol*. 2008;26:537–542. <https://doi.org/10.4067/S0717-95022008000300005>
  43. Rynn C, Wilkinson CM, Peters HL. Prediction of nasal morphology from the skull. *Forensic Sci Med Pathol*. 2010;6:20–34. <https://doi.org/10.1007/s12024-009-9124-6>
  44. Sforza C, Grandi G, De Menezes M, Tartaglia GM, Ferrario VF. Age- and sex-related changes in the normal human external nose. *Forensic Sci Int*. 2011;204:205.e1–205.e9. <https://doi.org/10.1016/j.forsciint.2010.07.027>
  45. Chen F, Chen Y, Yu Y, Qiang Y, Liu M, Fulton D, et al. Age and sex related measurement of craniofacial hard thickness and nasal profile in the Chinese population. *Forensic Sci Int*. 2011;212:272.e1–272.e6. <https://doi.org/10.1016/j.forsciint.2011.05.027>
  46. Schlager S, Rüdell A. Analysis of the human osseous nasal shape-population differences and sexual dimorphism: Human osseous nasal shape. *Am J Phys Anthropol*. 2015;157:571–581. <https://doi.org/10.1002/ajpa.22749>
-